Journal of Optoelectronics and Advanced Materials Vol. 5, No. 1, March 2003, p. 217 - 226

*INVITED PAPER*

# EASY AXIS DISTRIBUTION IN MODERN NANOPARTICLE STORAGE MEDIA: A NEW METHODOLOGICAL APPROACH

V. Kuncser*, W. Keune[a], M. Vopsaroiu[b], P. R. Bissell[b], B. Sahoo[a], G. Filoti

National Institute for Materials Physics, PO Box MG 7, 76900 - Bucharest-Magurele, Romania
[a]Laboratorium für Angewandte Physik, Gerhard-Mercator-Universität, 47048, Duisburg, Germany
[b]University of Central Lancashire, Magnetic Materials Research, Preston, PR1 2HE, UK

Easy axis distribution in metal particle magnetic tapes for linear digital data storage were studied by Mössbauer spectroscopy and magnetometry, for comparison. Qualitative and quantitative agreement between the distribution parameters deduced at room temperature via the two different techniques was found. The proposed methodology based on the interpretation of the Mössbauer data has the advantage that it can be applied at different temperatures and for very thin films. Moreover, angular spin distribution at low temperatures were obtained by Mössbauer spectroscopy and discussed with respect to the room temperature results. There was evidenced that the room temperature easy axis angular distribution contains both static orientation and dynamical components.

(Received July 20, 2002; accepted after revision March 12, 2003)

*Keywords*: Metal particle magnetic tapes, Easy axis distribution, Mössbauer spectroscopy, Magnetometry

## 1. Introduction

A special class of magnetic information storage media, namely the particulate media, has shown a continuously growing interest, due to a very basic recording principle and very low costs. When data density requirements were increased, the metal particle (MP) have replaced the oxide particle based storage media, imposing the advantage of higher saturation magnetisation for lower particle dimension [1]. Among them, elongated iron based metal particles provide large remanent magnetisation and coercivity. Such particles have to be stabilized against atmospheric oxidation by a careful passivation and various protective coatings. Unfortunately, even a passivation layer of a few nanometers can reduce the average magnetisation of the particles to one half of the bulk values. Even under these conditions, the MP systems present still superior performances compared with the iron oxide or cobalt-modified oxide particle systems [2,3].

Advanced MP tapes are now manufactured using double coating technologies which involve usually a thin magnetic layer superposed on a non-magnetic undercoat [1]. A magnetic field is applied during the polymer drying process, in order to increase the alignment of the particle easy axis, with large benefit to the storage performances. Increasing the magnetic texture, the squareness of the hysteresis loop becomes higher and the switching field distribution becomes narrower. In turn, the degree of magnetic texturing is very dependent on the technological procedures, e.g. the polymer viscosity, the rate of drying or the magnitude of the magnetic field. Therefore, the mapping of the easy axis distribution (EAD) in such materials is an important task devoted to the control of the manufacturing achievements.

The degree of magnetic texture is described by a three-dimensional distribution. Due to the preparation conditions and the geometry of the system, a much narrower out-of-plane angular

* Corresponding author: kuncser@alpha2.infim.ro

dispersion of the particle magnetic moment is expected, compared with the in-plane dispersion. Standard vibrating sample magnetometer (VSM) measurements are usually used in order to establish the EAD. In principle, both the in-plane and out-of-plane EAD may be obtained starting from Orientation Ratio (OR) measurements. As we will see in the following, this procedure can be effectively used for very narrow distributions and therefore, only the out-of-plane component of the EAD may be obtained in this way in some limiting cases [4]. However, the out-of-plane EAD is difficult to be deduced magnetically with reasonable accuracy due to demagnetisation effects. The in-plane EAD can be directly measured by using different techniques derived from Flanders and Shtrikman's principles [5]. It is worth mentioning that the complex magnetometric measurements used for the determination of EAD can be usually performed only at room temperature. We propose a new suitable technique and methodology for mapping the full EAD (both in-plane and out-of-plane components) in this kind of samples over a large range of temperatures. The methodology is based on the interpretation of the magnetic Mössbauer spectra taken in both perpendicular and non-perpendicular geometry. Moreover, some last achievements related to the evaluation of the EAD via magnetic measurements are discussed in a simple way. The experimental results obtained by magnetometry and Mössbauer spectroscopy on four different MP tapes are compared and the advantages of each technique are briefly presented.

## 2. Experimental details

The four analyzed samples of commercially produced double-coated MP tapes for digital data storage applications present a magnetic layer and a non-magnetic underlayer. The non-magnetic underlayer consist of nanoparticels of $\alpha$-$Fe_2O_3$ , with antiferromagnetic behavior at room temperature (RT), as suggested by both magnetic and Mössbauer measurements [6]. The magnetic layer contains ellipsoidal particles of metallic iron doped with a small amount of Co in order to increase the coercivity. The ellipsoids present an aspect ratio of 1:5 and a length of approximately 100 nm. The particles have been passivated at the surface and subsequently uniformly distributed in a non-magnetic polymer matrix. The embedding process has been done in the presence of a longitudinal applied field, in order to orient the ellipsoids with their easy axis along the tape length. The size distribution of the nanoparticles in both the magnetic and non-magnetic layers is very similar in all four samples. The only difference between the studied tapes is the thickness of the magnetic layer.

Bi-axial VMS experiments were carried out at room temperature to evaluate the in-plane and out-of-plane easy axis distributions. Experimental samples were prepared by stacking sixteen 1-cm diameter tape disks in order to increase the signal to noise ratio to a satisfactory level without compromising the sheet demagnetization factor of the samples.

Supplementary Mössbauer spectroscopy was used in order to derive the two components of the EAD. The spectra were acquired in both perpendicular and non-perpendicular geometry and at different temperatures by inserting the samples in a variable temperature bath cryostat. A $^{57}Co$ source in Rh matrix was used.

## 3. Results and discussion

### 3.1. Easy axis distribution obtained by magnetic measurements

A crude estimation of the texture effect can be obtained via the orientation ratio (OR). This is defined as the ratio of the remanent magnetisation along the recording direction (maximum probability for the EAD) and the remanent magnetisation along the transverse direction. Let us suppose that the sample is oriented with the maximum EAD along the Ox axis (see Fig. 1). After saturating the sample in a field H applied along Ox, the magnetic moments of the particles in the remanence state will relax back, respecting the configuration of the EAD (Fig. 1, upper). Contrary, if the field is applied transversely to the maximum EAD, namely along the Oy axis, the minimum energy of the magnetic moment system in the remanence state will require a new configuration and those spins, initially opposite to the magnetic field (quadrant IV in Fig. 1, lower), reorient by

respecting the field, namely along the same easy axis, but switched by 180° (quadrant II, Fig. 1, lower). We consider in the following that: (i) a two-dimensional component (either in-plane or out-of-plane) of the EAD is described by a distribution f(α), giving the probability that the magnetic moments of the nanoparticles point to the angle α relative to the direction of maximum probability, (ii) the distribution is symmetric about Ox and (iii) is relatively narrow (sharply decreasing probabilities towards ± π/2). Therefore, the orientation ratio can be expressed as:

$$OR = \frac{M_{Ox}^{r}}{M_{Oy}^{r}} = \frac{\int_{-\pi/2}^{\pi/2} f(\alpha)\cos\alpha d\alpha}{\int_{0}^{\pi/2} f(\alpha)\sin\alpha d\alpha + \int_{\pi/2}^{\pi} f(\alpha-\pi)\sin\alpha d\alpha} = \frac{\int_{0}^{\pi/2} f(\alpha)\cos\alpha d\alpha}{\int_{0}^{\pi/2} f(\alpha)\sin\alpha d\alpha} \quad (1)$$

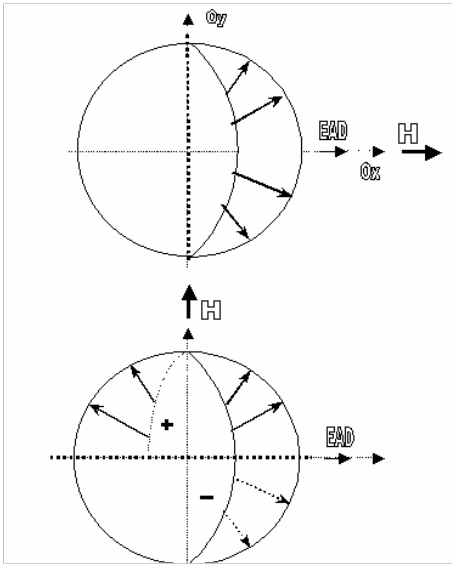


Fig. 1. Schematic representation of the magnetic moment orientation in the remanence state after removing a saturation field along Ox (upper) and Oy(lower), respectively.

The orientation ratio may be numerically estimated vs. parameters of the distribution f(α). In the case of a Lorentzian-like distribution, namely:

$$f(\alpha) = \frac{c(w/2)}{\alpha^2 + (w/2)^2} \text{ with the constant "c" derived from } \int_{-\pi/2}^{\pi/2} f(\alpha)d\alpha = 1 \quad (2)$$

the orientation ratio presents an exponential regression vs. the distribution width, *w*, [7], with an inferior asymptotic value of 1.5 and a sharper increment for distribution widths lower than a critical value, $w_c$ , of about 40° (OR ≅ 2.5 corresponds to $w_c$ ). Consequently, only distributions with $w < w_c$ may be estimated with a certain accuracy by this method. On the other hand, it has to be mentioned that both in-plane or out-of plane narrow EAD (with Oy in the tape plane and perpendicular to the tape plane, respectively) are suitable to be estimated in this way.

The orientation ratios are experimentally obtained by taking longitudinal and transversal hysteresis loops (either in-plane or out-of-plane) and estimating their remanence. Special care has to be taken to the demagnetising field corrections for the out-of-plane loops. Some magnetic data obtained on the analysed samples are presented in Table 1, where Mrt represents the remanent magnetisa-tion per unit volume multiplied by the effective magnetic coating thickness and $H_c$ is the coercive field, both deduced from longitudinal in-plane and out-of-plane hysteresis loops. It may be observed that out-of-plane components respect the condition of OR > 2.5, whereas the in- plane OR

are below this critical value. Therefore, reliable information about the EAD can be obtained only for the out-of-plane component. In this respect, the deduced values for the parameter *b=w/2*, describing the out-of-plane distribution, are 15(2)°, 15(2)°, 16(2)° and 18(2)° for samples A, B,C and D, respectively.

Table 1. Magnetic parameters of the analysed samples, obtained from VSM measurements.

| Sample | Mrt | $H_C$ | OR | |
|---|---|---|---|---|
| | (memu/cm$^2$) | (T) | out-of-plane | in-plane |
| A | 3.0 | 0.194 | 3.1 | 2.3 |
| B | 4.0 | 0.192 | 2.92 | 2.2 |
| C | 4.5 | 0.192 | 2.89 | 2.3 |
| D | 6.0 | 0.191 | 2.55 | 2.2 |

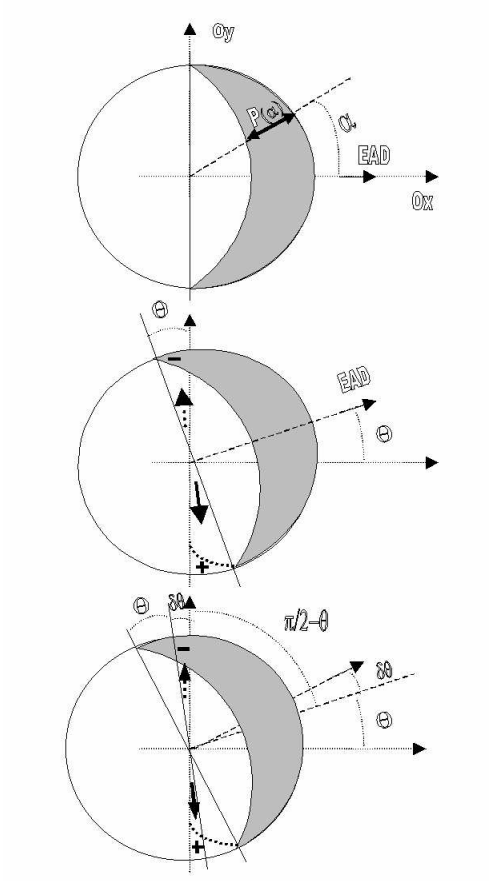


Fig. 2. Schematic representation of the magnetic moment orientation in the remanence state after removing a saturation field along Ox and rotating the sample by different angles vs. Ox: 0°(upper), θ (middle) and θ +dθ (lower).

Concerning the in-plane EAD component, this can not be suitably deduced from the orientation ratio and, therefore, other methods should be applied. In the following, a procedure for the evaluation of the in-plane component of EAD by a bi-axial VSM technique will be briefly described. Let us suppose a sample with the maximum of the in-plane EAD distribution along the Ox axis. After saturating the sample in a field parallel to Ox, the magnetic moments at remanence will respect the

initial EAD related to the Oxy system (Fig. 2, upper). The sample is turned by an angle θ relative to Ox and then saturated in a field applied also along Ox. The minimisation of the magnetic energy after removing the field (at remanence) will require particle magnetic moments with negative Ox projections to be switched by 180° along the same easy axis, resulting in Ox components along the field (Fig. 2, middle). Consequently, the magnetic moments introduced in quadrant II by the sample rotation will switch to their opposite directions into quadrant IV, inducing a change in the transverse remanent magnetisation (along Oy). At an additional infinitely small rotation, dθ, after saturating the sample and removing the field, the new magnetic moments introduced in quadrant II by the dθ rotation will switch again into quadrant IV(Fig. 2, lower). Because the switching moments are oriented at an angle π/2-θ with respect to the direction of maximum EAD probability, the infinitely small variation in the transverse remanent magnetisation induced by the small dθ rotation may be easily expressed as:

$$dM_{Oy} = 2 f(\pi/2 - \theta) d\theta \cos(d\theta/2) \tag{3}$$

With $d\theta \rightarrow 0$, $\cos(d\theta/2) \approx 1$, a π/2 shifted easy axis distribution, f(θ), may be obtained by the derivative of the transverse remanent magnetisation measured with a bi-axial VSM:

$$f(\pi/2 - \theta) \propto \frac{dM_{Oy}}{d\theta} \tag{4}$$

It is worth mentioning that the direction of the maximum in-plane component of the EAD related to a tape reference is found at the maximum remanence in the Ox direction (field direction), reached by the rotation of the sample at different angles θ. In the present case it corresponds strictly to the direction of the applied magnetic field during the polymer drying process. The experimental dependence for the derivative of the π/2 shifted transverse magnetisation of sample D is shown in Fig. 3. It results in a direct experimental evidence for a Lorentzian-like distribution [eq. (2)], for the in-plane component of the EAD. The following *b=w/2* - parameters were obtained by fitting the experimental points with such a dependence: 32(2)°, 27(2)°, 24(2)° and 21(2)° for samples A, B, C and D respectively. A clear decreasing trend of the distribution width vs. the Mrt values, namely vs. the effective thickness of the magnetic layer is observed. This effect should be related to the preparation conditions of the analysed magnetic tapes.

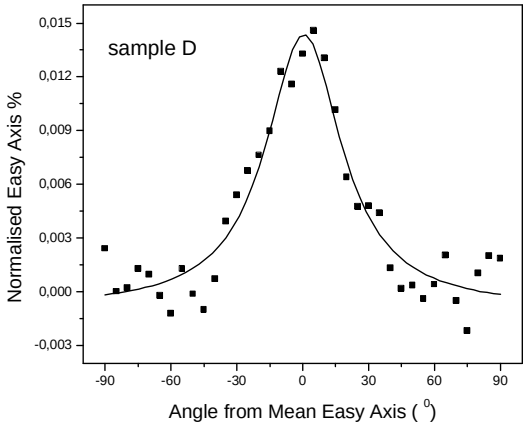


Fig. 3. Experimental in-plane EAD for sample D, obtained by the bi-axial VSM technique.

### 3.2. Easy axis distributions obtained by Mössbauer Spectroscopy

Since most of the magnetic recording media contain iron-based compounds, $^{57}$Fe Mössbauer spectroscopy represents a powerful tool providing both the nanoparticle magnetic moment orientation as well as the particle morphology or the magnetic phase distribution in particulate storage media [8,9]. Nevertheless, the Mössbauer study of the magnetic texture in such systems is based on a peculiar behavior. Because each nanoparticle represent a magnetic monodomain, all the atomic magnetic moments are oriented in the same direction and, consequently, the resulting particle magnetic moment is parallel with any atomic moment in that particle. Therefore, a microscopic method (as Mössbauer spectroscopy) giving the atomic spin orientation is finally able to provide the magnetic texture of the nanoparticle system. In Mössbauer spectroscopy, the spin configuration can be analyzed starting from the intensity ratio between the second (or fifth) and the third (or fourth) line, $R_{23} = I_2/I_3$, of the Zeeman-split Mössbauer sextet [10]. If the hyperfine field (which is anti-parallel to the spin direction) of an Fe atom is directed at an angle $\psi$ vs. the Mössbauer $\gamma$-ray direction, then $R_{23}=4\sin^2\psi/(1+\cos^2\psi)$. The out-of-plane spin component may be easily obtained from a Mössbauer spectrum in perpendicular geometry, the angular spin orientation vs. the sample plane being equal to $\pi/2-\psi$. Contrary, the above formula shows that the intensity ratio is insensitive to the in-plane spin directions ($R_{23}$ = 4) and, therefore, the in plane spin distribution may be analysed only in non-perpendicular geometry, with the $\gamma$-radiation incident at an angle $\phi$ vs. the sample plane. If the spin direction follows a certain angular distribution, $P(\varphi)$ , in the sample plane (where $\varphi$ is the in-plane azimuthal angle), the intensity ratio may be expressed by the relationship[11]:

$$R_{23} = 4\int_0^{2\pi} \frac{1-\cos^2\phi\cos^2\varphi}{1+\cos^2\phi\cos^2\varphi} P(\varphi)d\varphi \qquad \text{with} \qquad \int_0^{2\pi} P(\varphi)d\varphi = 1 \tag{1}$$

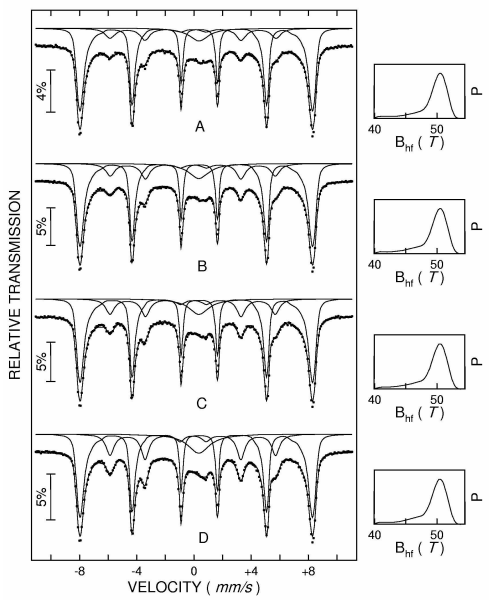


Fig. 4. RT Mossbauer spectra of the analysed samples, taken in perpendicular geometry. Right- hand side: corresponding hyperfine field distributions $P(B_{hf})$ of the $\alpha$-$Fe_2O_3$ underlayer.

The above intensity ratio can be theoretically evaluated for different model spin distributions as a function of the distribution parameters and the relative orientation between the sample and the $\gamma$-radiation. The distribution parameters are evaluated by equating the theoretical expression to the experimental intensity ratio for a number of experimental values equal to the number of the distribution parameters. The detailed procedure as well as numerical estimations of the intensity ratio

vs. parameters of the most common spin distributions (unidirectional, step-shaped and ellipsoidal-type) were presented in [11].

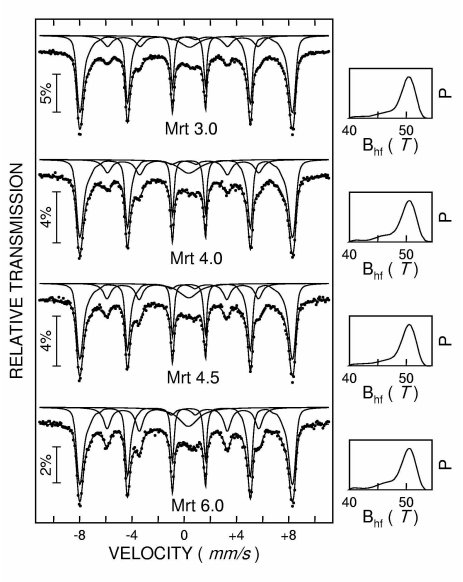


Fig. 5. RT Mössbauer spectra of the analysed samples with the radiation incident at 30° on the sample plane and the maximum EAD along the radiation. Right - hand side: corresponding hyperfine field distributions $P(B_{hf})$ of the $\alpha$-$Fe_2O_3$ underlayer.

Mössbauer spectra of the four analysed samples, taken at room temperature (RT) and in perpendicular geometry are presented in Fig. 4. They consist of two components: a sextet with a large Zeeman spliting and broad lines belonging to a defected antiferromagnetic $\alpha$-$Fe_2O_3$ phase (nanoparticles from the "non-magnetic" under- layer) with a hyperfine field around 49 T, and a less split sextet with a hyperfine magnetic field around 35 T, assigned to the $\alpha$-Fe(Co) metallic phase from the magnetic layer [6]. The central less pronounced paramagnetic phase is assigned to oxide nanoparticles with very small size, presenting superparamagnetic behaviour at RT. The suitable fitting of these spectra (unique hyperfine field for the iron positions in $\alpha$-Fe(Co) and hyperfine field distribution for the iron positions in $\alpha$-$Fe_2O_3$ nanoparticles) provides the experimental $R_{23}$ intensity ratio for the less-split sextet belonging to the nano-metal-particles. This can be used for evaluating the out-of-plane component of the particle magnetic moments. Subsequently, Mossbauer spectra were taken in non-perpendicular geometry, with the radiation incident at 30° on the sample plane and with the direction of the maximum EAD along the projection of the $\gamma$ radiation in the sample plane (Fig. 5). The $R^*_{23}$ intensity ratios (experimental intensity ratios obtained in non-perpendicular geometry and corrected by the influence of the out-of-plane spin component in agreement with [11]) of the inner sextet belonging to $\alpha$-Fe(Co) metallic nanoparticles, are presented together with $R_{23}$ (obtained in perpendicular geometry) in Table 2. Based on these results and following the numerical estimations of the intensity ratio for both the step-shape and the ellipsoidal distribution model[11], were finally obtained the corresponding parameters of the two distributions, $2\varphi$' and 2b' . It is worth mentioning that in the step-shape distribution model, the spins are supposed to be uniformly distributed into an angular aperture of $2\varphi$', symmetrical to the longitudinal field applied during the drying process, whereas in the ellipsoidal model, for not too wide-spread EA directions, the ellipsoidal distribution approaches a Lorentzian-like distribution, with the width at half maximum of 2b'. These two parameters, as well as the 2b parameters obtained by magnetic measurements, are presented in Table 2. The way by which the distribution parameters are obtained from the $R_{23}$ intensity ratios is briefly presented in Fig. 6 under the assumption of a step-shape distribution for the out-of-plane component of EAD. It consists in two steps: (i) the theoretical dependence of the intensity ratio vs. the

distribution parameter is evaluated within the assumed distribution and (ii) the distribution parameter is obtained from the theoretical curve by using the corresponding experimental intensity ratio as the ordinate.

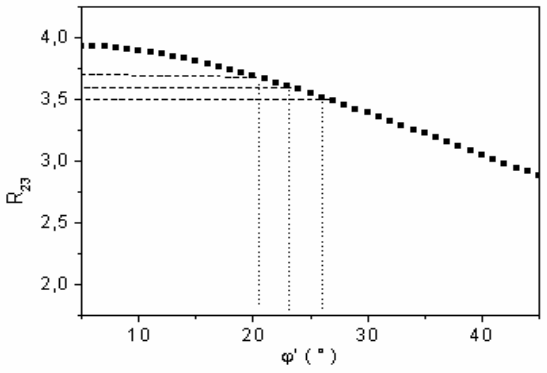


Fig. 6. Theoretical evolution of the intensity ratio for a geometry suitable to the derivation of the out-of- plane EAD. The step-shaped distribution model was assumed.

It may be observed from Table 2 that within the step-shape model the Mössbauer derived values for the aperture 2φ' are substantially higher that the parameters 2b' of the ellipsoidal distribution. The agreement between the Mössbauer and the magnetic measurements is quite good for similar distributions, namely Lorentzian-like in magnetic measurements and ellipsoidal type (which transforms into a Lorentzian-like distribution for eccentricities higher than 0.7, as in the case of the present measurements) in Mössbauer measurements.

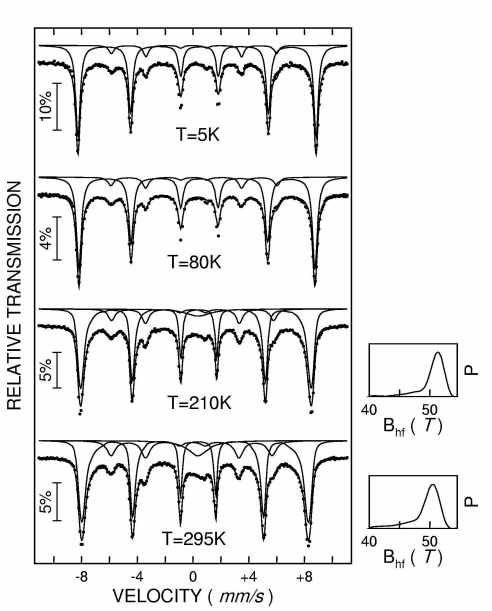


Fig. 7. Mössbauer spectra of sample C, taken in perpendicular geometry and at different temperatures. Right - hand side: corresponding hyperfine field distributions $P(B_{hf})$ of the α-$Fe_2O_3$ underlayer.

Table 2. Mössbauer intensity ratios and distribution parameters obtained by different techniques. Two models were assumed for the interpretation of the Mössbauer data.

| Sample | In-plane EAD component | | | | Out-of-plane EAD component | | | |
|---|---|---|---|---|---|---|---|---|
| | $R^{*}_{23}$ | 2φ' (°) | 2b' (°) | 2b (°) | $R_{23}$ | 2φ' (°) | 2b' (°) | 2b (°) |
| A | 2.90(5) | 103(3) | 56(3) | 65(3) | 3.60(5) | 46(3) | 29(3) | 30(3) |
| B | 3.10(5) | 80(3) | 47(3) | 55(3) | 3.70(5) | 42(3) | 27(3) | 30(3) |
| C | 3.20(5) | 80(3) | 43(3) | 48(3) | 3.50(5) | 52(3) | 32(3) | 32(3) |
| D | 3.35(5) | 70(3) | 40(3) | 42(3) | 3.60(5) | 46(3) | 29(3) | 36(3) |

### 3.3. Static vs. dynamic aspects of EAD

An additional advantage of Mössbauer spectroscopy over the magnetic techniques giving the EAD is related to the study of the spin relaxation behavior and the thermally induced component of the EAD. This can be obtained from temperature dependent Mössbauer spectra. Mössbauer spectra of sample C, collected in perpendicular geometry at four different temperatures are presented in Fig.7. The low temperature Mössbauer spectra show clearly only two magnetic sextets with narrow absorption lines. By increasing the temperature, the absorption lines of the outer sextet become broader (clear indication of the collective excitation regime for the oxide nano-particles) and a new central paramagnetic pattern is coming out above 150 K. At higher temperatures the Mössbauer spectra can be suitably fitted only with a hyperfine field distribution for the outer sextet belonging to the nano-oxide particles. Because the fit can not be unitarily done over the whole range of temperature, were considered as reliable only the parameters obtained by fitting the spectra either at temperatures lower than 100 K (Lorentzian sextets) or higher than 200 K (hyperfine field distribution for the outer sextet). The evolution of the $R_{23}$ intensity ratios for the inner sextet, assigned to the α-Fe(Co) nanoparticles, and the evolution of the absorption linewidth vs. temperature are presented in Fig. 8 and Fig. 9 respectively. Both an individual and overall decreasing trend for the intensity ratio of the analysed samples, simultaneously with increasing trend of the absorption linewidths may be seen. In this respect, linewidths of about 0.7 mm/s in the spectra acquired at RT can be related only to thermally induced hyperfine field distributions due to the collective excitations of the particle magnetic moments.

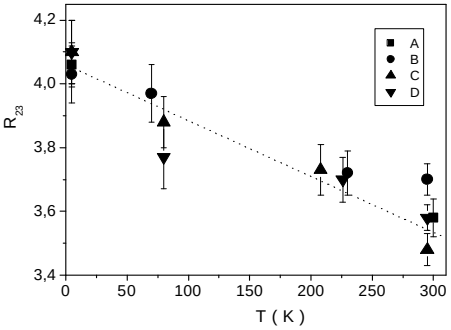


Fig. 8. The intensity ratio of the α-Fe(Co) Mossbauer component in the analysed samples, at different temperatures.

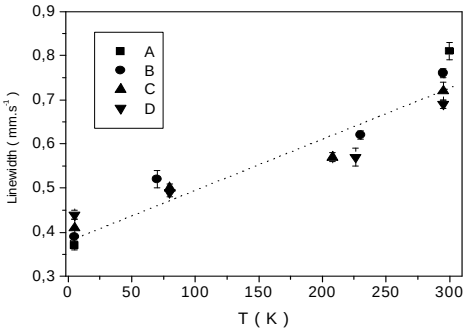


Fig. 9. The absorption linewidth of the α-Fe(Co) Mossbauer component in the analysed samples, at different temperatures.

The higher the magnetic moment thermal fluctuations, the higher is the out of plane mean component of the magnetic moment and the smaller is the $R_{23}$ intensity ratio. The intensity ratio at 5 K is 4.0 within the error bar limits, standing for perfect in-plane aligned magnetic moments. Values of about 3.6 for the intensity ratio at RT are interpreted as due to thermal fluctuations of the particle magnetic moments only. These fluctuations should present cylindrical symmetry around the direction

of maximum EAD and, therefore, the broader in-plane component of the EAD is expected to include similar dynamical effects.

## 4. Conclusions

EAD in four MP tapes for linear digital data storage were studied in a first step by magnetometry. The out-of-plane component of EAD was obtained via orientation ratio measurements, whereas the in plane component by a bi-axial VSM technique.

A new methodology for studying the EAD in such materials via Mössbauer spectroscopy was proposed. The out-of-plane component of the EAD may be obtained by Mössbauer experiments in perpendicular geometry, whereas the in-plane spin component is found via Mössbauer experiments in non-perpendicular geometry at different azimuth angles between the anisotropy main axis and the incident γ-ray direction. Mössbauer spectroscopy can provide the EAD at different temperatures and under different applied fields. Moreover, angular spin distributions correlated with the Fe phase composition at interfaces or in very thin films may be obtained by using back-scattering Mössbauer techniques, such as the Conversion Electron Mössbauer Spectroscopy (CEMS). The limitation imposed by this procedure is related to the fact that only the specific parameters of an apriori proposed type of distribution may be derived, but not the distribution shape. The shape of the real in-plane angular distribution component may be obtained in some limiting cases by bi-axial VSM techniques.

Two types of angular spin distribution were considered for the Mössbauer evaluations, namely the step-shape distribution and the ellipsoidal one. Good quantitative agreement with the magnetically derived data is achieved for similar distributions. Both static and dynamic components of the spin orientation distribution were evidenced by Mössbauer experiments at different temperatures.

### Acknowledgements

Financial support of Alexander von Humboldt Stiftung is highly acknowledged by one of the authors (V.Kuncser). The authors also wish to thank U. von Hörsten for valuable technical assistance. Partial support by the Deutsche Forschungsgemeinschaft (SFB 491) is appreciated.

## References

[1] R. J. Veitch, A. Ilmer, W. Lenz, V. Richter, J. Magn. Magn. Mater **193**, 279 (1999).
[2] G. Akashi, Proc. of ICF 3, Centre for Academic Publications, Japan, pp. 548-552 (1981).
[3] R. Chubachi, N. Tamagawa, IEEE Trans. on Magn. vol. 20, pp. 45-47 (1984).
[4] J. W. Harrell, Y. Yu, Y. Ye, J. P. Parakka, D. E. Nikles, H. G. Zolla, J. Appl. Phys. vol. **8**, 8 (1997); P. R. Bissell, M. Vopsaroiu, R. D. Cookson, M. P. Sharrock, JEMS Conf. Aug. 2001, B001.
[5] P. J. Flanders, S. Shtrikman, J. Appl. Phys. **33**, 1 (1962).
[6] V. Kuncser, M. Vopsaroiu, B. Sahoo, P. R. Bissell, W. Keune, Proceed. Intern. Conf. on Applications of the Mossbauer Effect (ICAME 2001), Oxford, UK, Sept 2001, Hyp. Int (in press).
[7] M. Vopsaroiu, P. R. Bissel, V. Kuncser, W. Keune, submitted to J. Magn. Magn. Mat.
[8] M. P. Morales, K. O'Grady, S. Betteridge, D. P. E. Dickson, J. Magn. Magn. Mater. **155**, 129 (1996).
[9] F. T. Parker, F. E. Spada, T. J. Cox, A. E. Berkowitz J. Magn. Magn. Mater. **162**, 122 (1996).
[10] G. K. Wertheim, Mössbauer Effect: Principles and Applications, Academic Press, New York, (1964).
[11] V. Kuncser, W. Keune, M. Vopsaroiu, P. R. Bissell, Nucl. Instr. and Meth. in Phys.Res. B **196** 135 (2002).